

## PARAMETERS OF A GAS-POWDER FLOW FORMED BY A CUMULATIVE ACCELERATOR AND REALIZING THE EFFECT OF SUPERDEEP PENETRATION

O. V. Roman, S. K. Andilevko, and  
S. S. Karpenko

UDC 534.2

*The development of a gas-powder flow formed by an explosive accelerator with a cumulative recess in its lower part is numerically investigated. A comparative analysis of two variants of a cumulative system of impelling that are basic to the effect of superdeep penetration has been carried out, and their integral parameters have been estimated.*

Up to the present time, the effect of superdeep penetration has been obtained in the majority of cases using a system of acceleration and formation of a flux of powder particles [1, 2]: this system is known as a cumulative system (Fig. 1a). Direct experimental study of the parameters of the flow generated by such a system turned out to be impracticable. This is explained by the fact that because of the large number of metallic parts used in this system, a rather large flux of fragments which prevent normal functioning of the research equipment is formed after an explosion. Additional barriers to the experimental study of the flow are formed by one of the technological elements of the system – the regulating support (RS). This element is made from a thick-walled (up to 10 mm) metallic tube, which makes it opaque to optical equipment. On the other hand, the system of acceleration is too complicated for analytical modeling, and it abounds with a relatively large number of structural members and boundary surfaces. Thus, the only realistic method of detailed study of the parameters of the flux formed by a cumulative system is the use of calculational procedures which allow one to model the flow by numerical-experiment methods.

**Numerical Model.** The complex of programs for constructing the difference scheme of a numerical experiment is based on the method of "large particles" [3, 4]. In this case, the powder is considered as a hydrodynamic medium with parameters given by either a  $D-U$  adiabat or an equation of state [5]. Calculations done using relatively large cells whose size is much larger than the thickness of the detonation-wave front allow one to model the detonation in integral form regardless of the features of the processes occurring inside this front [6]. The compression of a "cold" explosive up to the moment of its explosion and the separation of detonation products are calculated using an equation of state [7]. Detonation is initiated in the cells filled with the explosive and positioned at a distance  $\leq Dt$  from the reference point at a given instant of time  $t$  if the pressure in them is higher than the critical pressure  $p_{cr}$  [8]. In this case, the internal energy of the initiated cell increases once by a value of  $Q$  corresponding to the explosion heat of the explosive used. The calculation is done by the method of "large particles" using a through difference scheme with rectangular whole cells that is adapted to cylindrical coordinates [3, 4]. The choice of the dimensions of the cells is limited by the requirements of convergence of the method, and the time step is determined by the dimensions of the cells [3]. The flow parameters used are expressed in dimensionless form. The units of the basic quantities were as follows: the detonation rate  $D$  ( $\sim 4000$  m/sec for ammonite 6 ZhV) was taken as a unit of

---

Scientific-Research Institute of Pulsed Processes, Belarusian State Science and Production Concern of Powder Metallurgy, Minsk, Belarus. Translated from *Inzhenerno-Fizicheskii Zhurnal*, Vol. 74, No. 2, pp. 73–78, March–April, 2001. Original article submitted August 3, 2000.

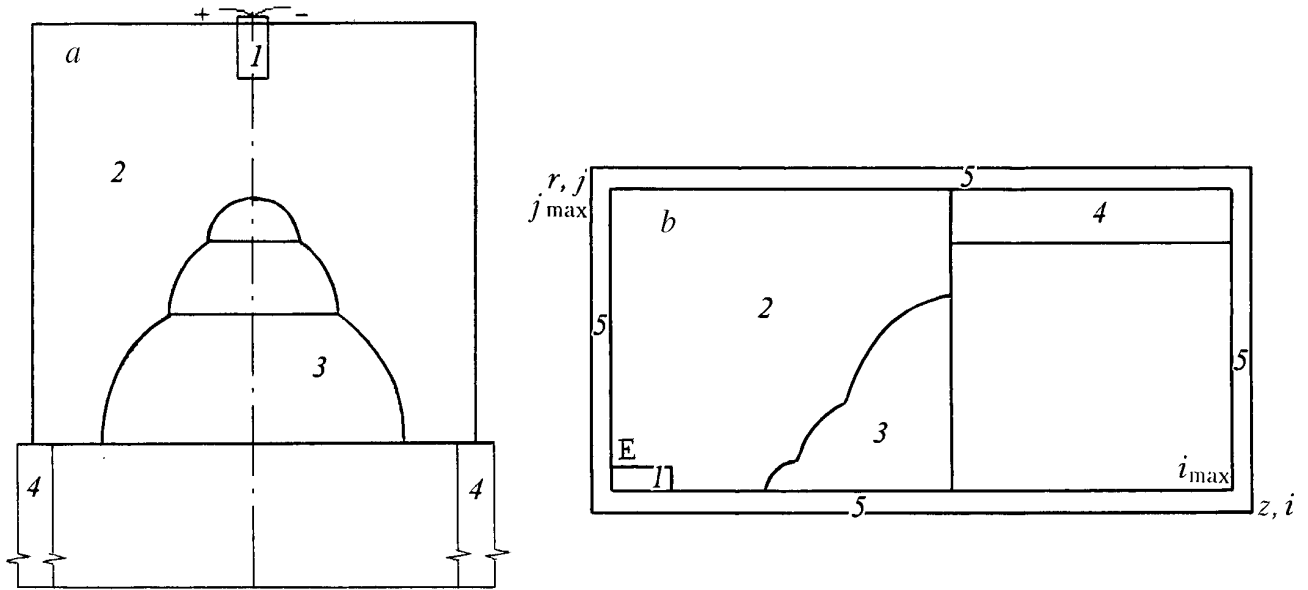


Fig. 1. Technical (a) and calculated (b) systems of an explosive accelerator: 1) electric detonator; 2) explosive; 3) powder packing; 4) regulating support; 5) fictitious layer of calculation cells.

velocity, the explosive density  $\rho_e$  as a unit of density ( $\sim 1000 \text{ kg/m}^3$  for ammonite 6 ZhV), and the total length of the system  $L$  as a unit of length (in our case,  $L = 0.18 \text{ m}$ ). The running parameters are as follows:

$$z = \frac{\bar{z}}{L}, \quad r = \frac{\bar{r}}{L}, \quad U = \frac{\bar{U}}{D}, \quad V = \frac{\bar{V}}{D}, \quad t = \frac{\bar{D}}{L}t, \quad \rho = \frac{\bar{\rho}}{\rho_e}, \quad e = \frac{\bar{e}}{D^2}, \quad p = \frac{\bar{p}}{\rho_e D^2}. \quad (1)$$

To provide fulfillment of the boundary conditions, around the entire calculation field (Fig. 1b) we formed a layer of fictitious cells [9, 10] with the following numbers: 0 and  $j$  ( $j = 1, 2, \dots, j_{\max}$ , where  $j_{\max}$  is the maximum number of actual cells in the radial direction) on the left,  $i_{\max} + 1$  and  $j$  ( $i_{\max}$  is the maximum number of actual cells in the axial direction) on the right,  $i$  and  $j_{\max} + 1$  over the side surface (Fig. 1b, at the top), and  $i$  and 0 along the symmetry axis (Fig. 1b, at the bottom). On the left end of the scheme and along the side surface (in the region where the regulating support is absent), we prescribed the condition of outflow into a vacuum

$$g_{0,j} = g_{1,j} \quad (2)$$

and

$$g_{i,j_{\max}+1} = g_{i,j_{\max}}, \quad (3)$$

where  $g = (e, \rho, U, V, p)$ . Along the axis of symmetry we determined the no-flow condition

$$s_{i,0} = s_{i,1}, \quad U_{i,0} = -U_{i,1}, \quad (4)$$

where  $s = (e, \rho, V, p)$ . As in an actual experiment, the test sample was positioned on the right end of the scheme. It is also necessary to assign the no-flow condition on the surface of the test sample:

$$w_{i_{\max}+1,j} = w_{i_{\max},j}, \quad V_{i_{\max}+1,j} = -V_{i_{\max},j}, \quad (5)$$

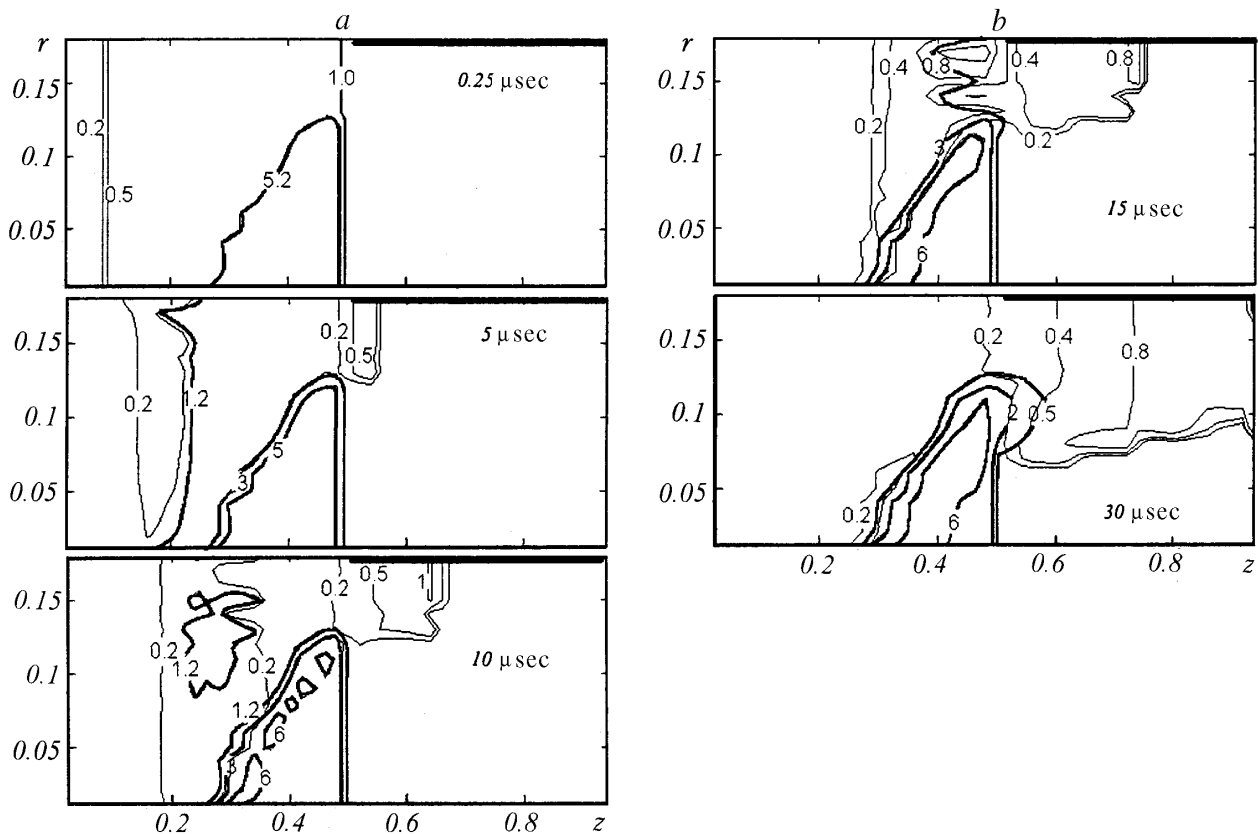


Fig. 2. Detonation of a charge and development of a shock wave in the powder (a), breakthrough of detonation products into the cavity of a regulating support and beginning of the peripheral destruction of the powder packing (b). The velocity isolines are denoted by the thin lines and the density isolines are denoted by the thick lines.

where  $w = (e, \rho, U, p)$ . In the cases where we calculated the system with a regulating support, the conditions of outflow into a vacuum were assigned only for the part of the scheme in which the regulating support was absent, and in the part with this support the radial component of the velocity on its surface changed its sign to the opposite. All the other quantities did not experience changes in the layer of fictitious cells.

The initial conditions were provided by a special "detonator": in the group of cells denoted as region  $E$  in Fig. 1b (3 cells in  $j$  and cells 5–6 in  $i$ ), the internal energy of the material was increased once by the value of  $Q$ , thus simulating the operation of an electric detonator. Then the calculations were done by a standard scheme in three steps according to the method of "large particles" [3, 4] with periodic output, graphic processing, and retaining of the data obtained. To simplify the observation of the moving boundary surfaces, the powder was separated from the explosive and air by a chain of moving markers [9, 10] that remained continuous throughout the period of calculation. The parameters of the air flow in the cavity of the regulating support were determined from the polytrope with an exponent of 1.4 for an initial density of  $1.23 \text{ kg/m}^3$ . For the model impelled material we used a bronze powder (the initial density was  $4830 \text{ kg/m}^3$ ), and for the explosive we used ammonite 6 ZhV.

The results of the calculations done using the given package of programs were compared with the analytical data on the parameters of motion of continuous bodies impelled by an explosion [9, 10], the experimental results obtained using the system without a regulating support [1], and the results of a special test experiment [11]. In all cases, we observed a quite satisfactory agreement among the compared data.

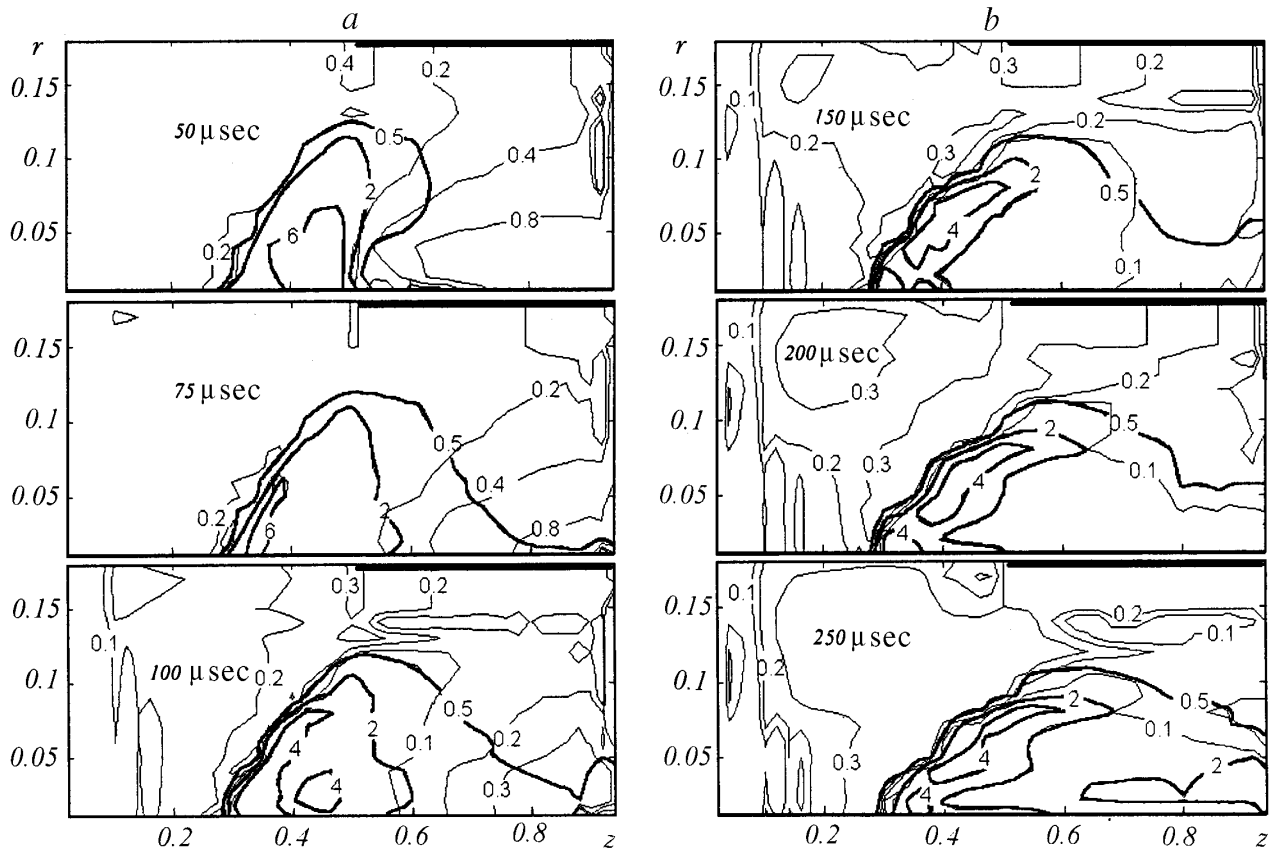


Fig. 3. Development of a jet at the early (a) and middle (b) stages of flow for the system of acceleration with a regulating support.

**Results of Calculations of a Standard System of Acceleration.** A standard system of impelling that is used in experiments on superdeep penetration comprises a cylindrical explosive charge with an axially symmetric recess (three joined hemispheres, Fig. 1a [2]) in its lower part, which is positioned at a distance from the treated sample. A system in which the acceleration is performed in the cavity of a thick-walled tube (the regulating support in Fig. 1a) is more often used in experiments; however, a system without a regulating support was also used in a number of works. The results of a numerical analysis have shown that to around the 46th  $\mu\text{sec}$ , the flow in a system with a regulating support and the flow in a system without a regulating support develop in the same manner. Since the total linear dimension of these systems is the same, the authors express the time intervals in terms of a dimensional quantity, and the reverse conversion can be performed by recognizing that  $1 \mu\text{sec} \approx 0.0222$  and  $45 \mu\text{sec} \approx 1.0$ . This acceleration period is shown in Fig. 2. Figure 2a illustrates the period of development of the flow behind the detonation wave, its emergence at the free surface of the charge, the breakthrough of the detonation product into the cavity of the regulating support, and the initial stage of propagation of the shock wave in the powder packing (the initial density of the bronze powder is  $4830 \text{ kg/m}^3$ , i.e., 4.83 in dimensionless quantities; values of the density  $\geq 5$  correspond to a compacted material). The velocity of the flow behind the shock-wave front is  $\sim 0.2$  ( $\sim 800 \text{ m/sec}$ ). Figure 2b shows the development of the flow behind the shock wave in the powder with formation of the "Mach lens" and the beginning of destruction of the peripheral surface of the powder packing. The velocity in this region continues to be small ( $\leq 0.2$ ). The detonation products broken through into the cavity of the regulating support form an axially symmetric (quasiconic) shock wave converging to the barrier axis. The interaction of this conic wave with the "Mach lens" results in the formation of a high-speed jet flow along the axis of symmetry (Fig. 3a,  $50 \mu\text{sec}$ ) that is characterized by a high velocity gradient in the axial direction. In Figs. 2–5, the

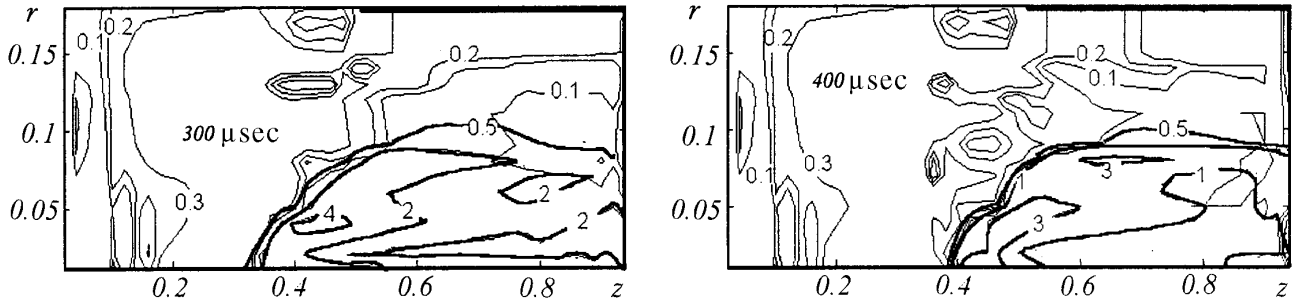


Fig. 4. Final stages of flow for the system of acceleration with a regulating support.

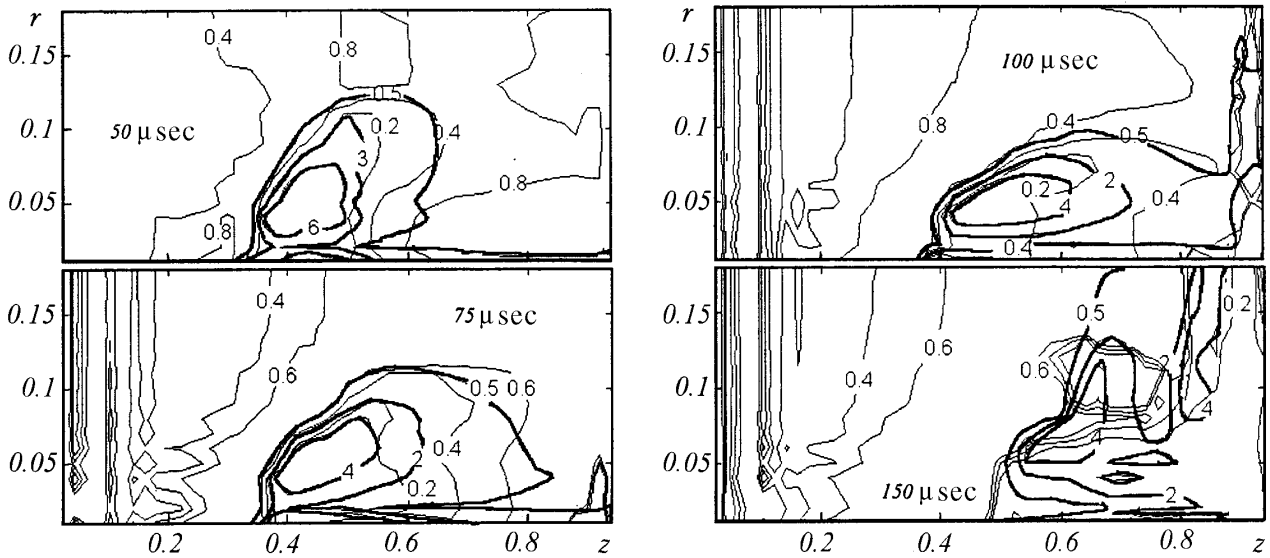


Fig. 5. Development of the gas-powder flux in the system of acceleration without a regulating support.

density isolines are denoted by the heavy lines, and the longitudinal-velocity isolines are denoted by the thin lines. In the process of development of this flow, a portion of the powder from the powder packing is involved in it, which brings about the formation of a gas-powder flux that reaches the surface of the test sample by the instant  $75 \mu\text{sec}$  (Fig. 3a). The density of this flux is relatively low, but it rapidly increases as the flux approaches the axis of symmetry. On the average, it is characterized by a value of  $0.75\text{--}0.8$ , which corresponds to  $750\text{--}800 \text{ kg/m}^3$ . Whereas at the instant  $\bar{t} = 75 \mu\text{sec}$  the flow velocity is  $0.85$  ( $3.2 \text{ km/sec}$ ) in the region of interaction with the barrier, at  $\bar{t} = 100 \mu\text{sec}$  it decreases to  $0.51$  ( $2.04 \text{ km/sec}$ ) for the same average density, and at  $\bar{t} = 150 \mu\text{sec}$ ,  $V \approx 0.22$  ( $880 \text{ m/sec}$ ) (Fig. 3b) for  $1.0 \leq \rho \leq 1.1$ . Then the velocity of the main mass of the material is equalized and approaches a value of  $0.1$  ( $400 \text{ m/sec}$ ). The increase in the flow density becomes marked (it is equal to  $1.3$  at  $200 \mu\text{sec}$  and  $2.25$  at  $250 \mu\text{sec}$ ). However, the flow velocity remains stationary and equal to  $\sim 0.1$ , and this tendency remains constant at a later time (Figs. 3b and 4).

The powder flow in a system without a regulating support begins to differ markedly from the powder flow in a system with a regulating support after  $43\text{--}44 \mu\text{sec}$  of the operation of an explosive accelerator. Before this time, the flows in these two systems develop in the same manner. This development is illustrated in Fig. 2. However, the high-speed jet arising in the system without a regulating support is initially more rapid than the analogous jet arising in the system with a regulating support (Fig. 5), and its first contact with the barrier takes place for a velocity of  $\sim 1.26$  ( $5040 \text{ m/sec}$ ) already at the  $48\text{th} \mu\text{sec}$ . The velocity gradient along the jet is rather high (from  $1.26$  to  $0.8$ ), and the density averaged over the interaction cross section is

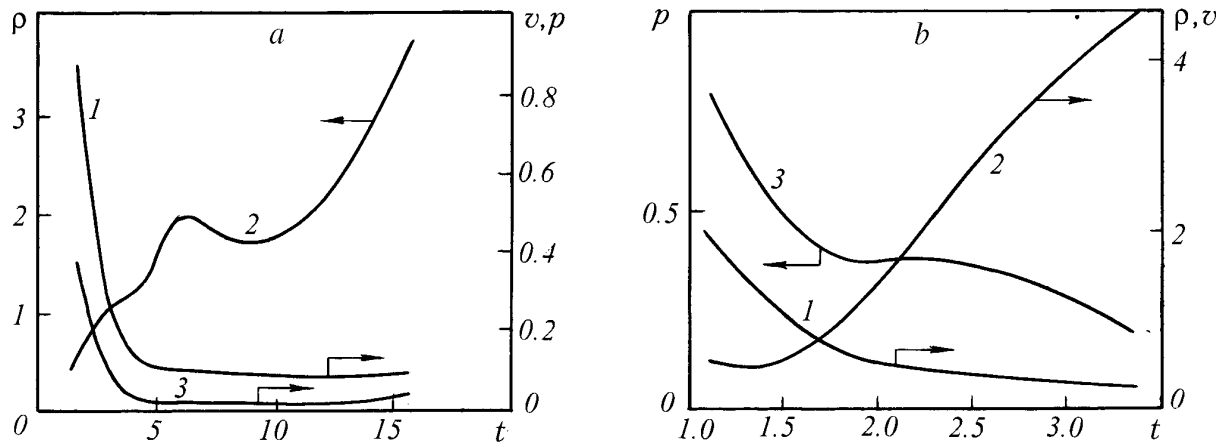


Fig. 6. Temporal changes in the velocity (1), density (2), and pressure (3) at the level of the sample surface for the system with a regulating support (a) and for the system without a regulating support (b).

TABLE 1. Temporal Changes in the Parameters of the Particle Flux Averaged over the Cross Section of Interaction with the Barrier

$\bar{t}$ , $\mu\text{sec}$	$T$	$V$	$\rho$	$p$	$R$	$S$
<i>With a regulating support</i>						
75	1.667	0.85	0.5	0.36125	0.015	0.000707
100	2.222	0.51	0.8	0.20808	0.048	0.007238
150	3.333	0.22	1.1	0.05324	0.052	0.008495
200	4.444	0.12	1.3	0.01872	0.052	0.008495
250	5.556	0.10	1.9	0.01900	0.052	0.008495
300	6.667	0.10	1.9	0.01900	0.055	0.009503
400	8.889	0.09	1.7	0.01377	0.057	0.010207
700	15.554	0.09	3.6	0.02916	0.059	0.010936
<i>Without a regulating support</i>						
50	1.111	1.26	0.5	0.7938	0.013	0.000531
75	1.667	0.77	0.7	0.4153	0.019	0.001134
100	2.222	0.43	2.0	0.3698	0.143	0.064240
150	3.333	0.21	4.5	0.1895	0.150	0.070680

$\sim 0.5$ . From this point on, the interaction of the flow with the barrier in the system without a regulating support proceeds at a higher rate than that in the system with a regulating support. In this case, the velocity of the main mass of the powder is also rather high (0.2–0.5). As a result, the time of interaction decreases cardinally; already at 160  $\mu\text{sec}$  the rate of the flow–barrier collision decreases sharply, and after 170  $\mu\text{sec}$  the axial component of the velocity near the barrier surface is practically equal to zero. The temporal changes in the averaged parameters of the flow in the region of interaction of the gas-powder jet with the sample are presented for both systems in Table 1 and in Fig. 6.

**Integral Parameters of the Impelling.** In investigating the processes involved in superdeep penetration, it is extremely important not only to know the hydrodynamic characteristics of the flux but also to have a complex idea of the level and character of its interaction with the barrier. For this purpose, in the program we reserved the possibility for accumulative calculation of the integral parameters of loading, to which we assigned the momentum and energy, which are transferred to the barrier by the flux, and the power with which the gas-powder flux acts on the barrier.

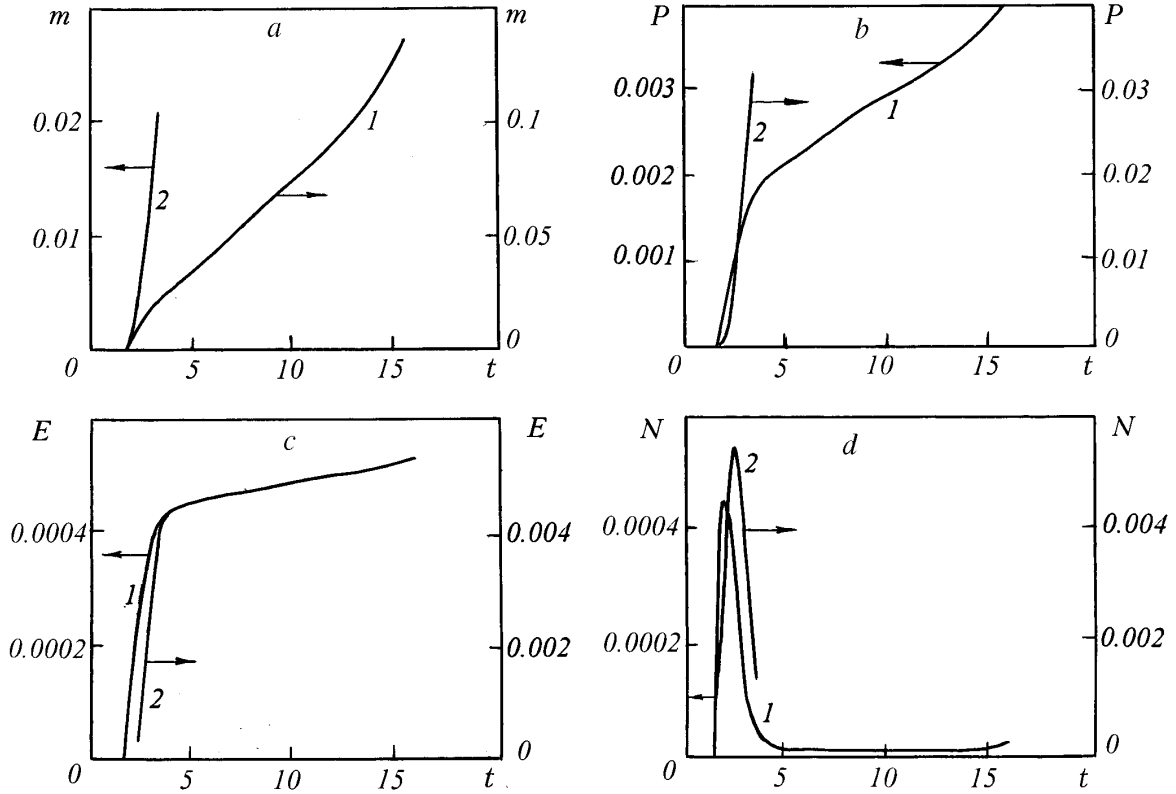


Fig. 7. Temporal changes in the mass (a), momentum (b), transferred energy (c), and power (d) of the flux in the cross section of interaction of particles with the barrier for the system of acceleration with a regulating support (1) and for the system without a regulating support (2).

TABLE 2. Total and Averaged Parameters of the Flux in Dimensional and Dimensionless (in parentheses) Quantities

System	$t_t, \mu\text{sec}$	$p_a, \text{GPa}$	$P_t, \text{kg}\cdot\text{m}/\text{sec}$	$N_a, \text{GJ}/\text{sec}$	$E_t, \text{MJ}$	$V_a, \text{m}/\text{sec}$	$\rho_a, \text{kg}/\text{m}^3$
With an RS	703	0.597	92.1	0.079	0.050	560	1882
	(15.64)	(0.037)	(0.004)	$(3.8\cdot 10^{-5})$	$(5.3\cdot 10^{-4})$	(0.14)	(1.882)
Without an RS	152.5	7.093	738.7	3.893	0.389	2448	2107
	(3.39)	(0.443)	(0.032)	(0.0019)	(0.0042)	(0.612)	(2.107)

The momentum  $P$  is transferred to the barrier by a flux in the interaction cross section 5, on condition that the deceleration of the flux is complete,  $P = mV_a$ , where  $V_a$  is the axial velocity averaged over the interaction cross section and  $m$  is its mass. The change in the momentum in this cross section within a small time interval  $dt$  ( $dt$  is sufficiently small to assume that the flux velocity is constant in this time interval)

$$dP = V_a dm = \rho S V_a^2 dt. \quad (6)$$

The dependence of the momentum on time is

$$P(t) = \int_0^t \rho(\tau) S(\tau) V_a^2(\tau) d\tau. \quad (7)$$

The energy transferred to the barrier by the flux can be determined from the dependence  $E = mV_a^2/2$ . Then the change in the energy (on condition that the velocity is constant in the interval  $dt$ ) is

$$dE = \frac{V_a^2}{2} dm = \rho S \frac{V_a^3}{2} dt, \quad (8)$$

whence it follows that

$$E(t) = \int_0^t \rho(\tau) S(\tau) \frac{V_a^3(\tau)}{2} d\tau. \quad (9)$$

The power with which the flux acts on the barrier is

$$N = \rho S \frac{V_a^3}{2}. \quad (10)$$

The results of the calculation of parameters (6)–(10) for the two systems of impelling are presented in Fig. 7. It is obvious that in the system without a regulating support the flux develops much more rapidly. Table 2 presents data on the averaged values of these quantities for the entire process of acceleration in a given concrete case (the corresponding dimensionless quantity is given in the parentheses). It is easy to verify that in the system without a regulating support the pressure is higher by more than an order of magnitude, the average rate of interaction is markedly increased (by a factor of 4.4), the power of the flux is practically 50 (49.2) times higher, and the quantity of energy transferred to the barrier is 7.8 times higher. The difference in functioning between these two systems of impelling is clearly supported by the experimental data. In both cases, we loaded stacks consisting of round aluminum plates with a diameter of  $\sim 60$  mm and a thickness of 2 mm that were assembled into a steel casing (a section of a tube). In the system without a regulating support, the jet broke through seven plates, leaving deep dents on the eighth and ninth plates, while in the system with a regulating support only the first plate was forced through (forced, but not broken through), and the dent made by the impact was seen even on the fifth plate.

The calculations performed allow one more important conclusion: in contrast to a conic explosive accelerator [11], in a standard scheme of acceleration (see Fig. 1a) the jet of the working material consists not of three main parts (high-speed jet, main mass, and pestle [11]), but of two. In this case, a pronounced high-speed jet is observed (Figs. 3a and 5), whereas the main mass of the material and the pestle practically merge together.

This work was carried out within the framework of a grant from the Belarusian Republic Basic Research Foundation, No. T98–199.

## NOTATION

$D$ , detonation rate;  $V$  and  $U$ , axial and radial components of the velocity;  $t$ , time;  $p$ , pressure;  $P$ , momentum transferred to the barrier by the flux;  $Q$ , explosion heat;  $e$ , energy of the flux;  $E$ , quantity of energy transferred to the barrier by the flux;  $L$ , total length of the system;  $r$  and  $z$ , radial and axial coordinates;  $R$  and  $S$ , radius and area of the contact spot on the surface of the treated barrier;  $g$ ,  $w$ , and  $s$ , local notation of the vectors;  $m$  and  $N$ , mass and power of the flux interacting with the barrier;  $\rho$ , density;  $\tau$ , integration variable. Subscripts:  $i$  and  $j$ , numbers of cells in the axial and radial directions, respectively; max, maximum value; cr, critical value; a, average; e, explosive; t, total (throughout the acceleration time) value; an overscribed bar denotes dimensional quantities in the SI system.



## REFERENCES

1. M. Jeandin, M. Vardavoulias, S. K. Andilevko, O. V. Roman, V. A. Shilkin, and S. M. Usherenko, *Rev. Metall.*, No. 12, 808–812 (1992).
2. S. M. Usherenko, *Superdeep Penetration of Particles into Barriers. Creation of Composite Materials* [in Russian], Minsk (1998).
3. O. M. Belotserkovskii and Yu. M. Davydov, *Method of Large Particles in Gas Dynamics. Computational Experiment* [in Russian], Moscow (1982).
4. O. M. Belotserkovskii, *Numerical Modeling in the Mechanics of Continuous Media* [in Russian], Moscow (1984).
5. A. P. Mirilenko, *Development of the Processes of Production of High-Density Billets from Difficult-to-Compact Powders by Explosion Compaction in Nonequilibrium Regimes*, Candidate's Dissertation in Technical Sciences [in Russian], Minsk (1990).
6. C. Mader, *Numerical Modeling of Detonation* [in Russian], Moscow (1985).
7. V. F. Kuropatenko, *Chisl. Metody Mekh. Sploshn. Sred*, **8**, No. 6, 68–71 (1977).
8. F. A. Baum, L. P. Orlenko, K. P. Stanyukovich, V. P. Chelyshev, and B. I. Shekhter, *Physics of Explosion* [in Russian], Moscow (1975).
9. S. K. Andilevko, *Superdeep Mass Transfer of Discrete Microparticles in Metallic Barriers under the Conditions of Loading of the Latter by a Powder Flux*, Candidate's Dissertation in Physical and Mathematical Sciences [in Russian], Minsk (1991).
10. S. K. Andilevko, G. S. Romanov, and S. M. Usherenko, *Inzh.-Fiz. Zh.*, **61**, No. 1, 46–51 (1991).
11. O. V. Roman, S. K. Andilevko, and O. A. Dybov, *Inzh.-Fiz. Zh.*, **73**, No. 4, 797–801 (2000).